Considering Avoidance and Consistency in Motion Planning for Human-Robot Manipulation in a Shared Workspace

Rafi Hayne, Ruikun Luo, and Dmitry Berenson
Worcester Polytechnic Institute
{rhhayne, rluo, dberenson}@wpi.edu

***Abstract*— This paper presents an approach to formulating the cost function for a motion planner intended for human-robot collaboration on manipulation tasks in a shared workspace. To be effective for human-robot collaboration a robot should plan its motion so that it is both safe and efficient. To achieve this, we propose two factors to consider in the cost function for the robot's motion planner: (1) Avoidance of the workspace previously-occupied by the human, so that the motion is as safe as possible, and (2) Consistency of the robot's motion, so that the motion is as predictable as possible for the human and they can perform their task without focusing undue attention on the robot. Our experiments in simulation and a human-robot workspace sharing study compare a cost function that uses only the first factor and a combined cost that uses both factors vs. a baseline method that is perfectly consistent but does not account for the human's previous motion. We find that using either cost function we outperform the baseline method in terms of task success rate without degrading the task completion time. The best task success rate is achieved with the cost function that includes both the avoidance and consistency terms.**

I. Introduction

While factory automation has been studied for many years, many manufacturing tasks have proven difficult to automate fully because they must be performed in close proximity to a human, or because parts of the task require human-level perception and/or manipulation capabilities not yet achievable by robots. To overcome this difficulty, a robot and human can collaborate to perform manufacturing tasks. However, when humans and robots share a workspace, the robot must be able to avoid interference with the human and potential collisions so that the task can be completed safely and efficiently.

A robot motion planning algorithm that is used in such a collaborative workspace must consider human safety and the human's expectations in the trajectories it produces. This paper investigates how to formulate a cost function for the robot's motion planner such that both safe and efficient task execution results. Two fundamental factors are considered in the formulation of the cost function: (1) Avoidance of the workspace previously-occupied by the human, and (2) Consistency of the robot's motion.

The first factor is motivated by our observations of humans collaborating on structured manipulation tasks where they are asked to repeatedly reach to the same areas in a shared workspace. After an initial period where the participants may try different strategies, their motion becomes very similar and they consistently enter the workspace of their partner with high speed while avoiding collision. We hypothesize that this behavior is akin to forming separate "lanes" that the humans move in. For instance one person may reach closer to the table (e.g. elbow down) while the other reaches over the first's arm (elbow up). In this paper we investigate if this apparent lane-forming can be exploited for human-robot workspace sharing tasks by biasing the robot's motion planner to avoid the lanes created by the human.

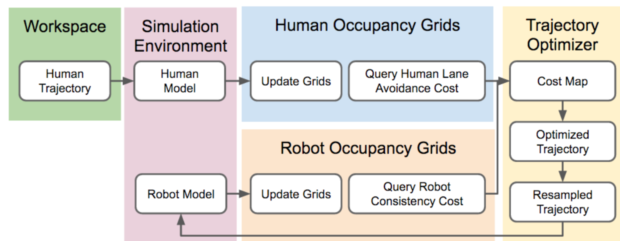

Fig. 1. Pipeline for the method. A human trajectory in the workspace is captured by a motion capture system. This data is sent to the simulation environment where an occupancy grid is updated. Finally, occupancy grids for both the human and robot are queried to generate two cost functions to be used in trajectory optimization. Planned trajectories are fed back into the occupancy grid to further describe robot lanes of traversal.

However, considering the first factor alone may not be sufficient because the human's motion is affected by their partner's motion. This necessitates considering the second factor: consistency. Again, considering this factor is motivated from observations of previous human-robot collaboration experiments: When the robot's behavior (or even the robot itself) is new to the human, the human tends to move very cautiously. We hypothesize that this is because the human finds the robot's motion difficult to predict. However, as the two continue to move in the same space for a consistent set of tasks, the human usually becomes bolder in their motion around the robot, increasing their velocity and exploiting free work space around the robot's motion. Thus we also consider the consistency of the robot's motion as part of the cost function. To produce more consistent motion, we bias the planner to move the robot through the same workspace it used previously. A central challenge in this work is representing both the avoidance and consistency factors using cost functions in a way that works well in the TrajOpt [1] trajectory optimizer we use for motion planning. We propose a human lane penetration cost function to enable the avoidance of the human and a robot self-lane cost function to bias the robot toward consistent motion.

Our experiments in simulation and a human-robot workspace sharing study compare a cost function that avoids only the human lanes and a combined cost that uses both factors vs. a baseline method that is perfectly consistent but does not account for the human's previous motion. An overview of our experimental framework is shown in Figure 1. We find that using either cost function we outperform the baseline method in terms of success rate of the human's task without degrading task completion time. The cost function that accounts for both avoiding the human's lane and the consistency of the robot's motion has the best success rate. These results suggest that our method produces collaborations that interfere less with the human, allowing humans to move with less error and therefore making the task execution more efficient.

The remainder of this paper describes related work, the implementation of the cost functions and their use in the TrajOpt motion planner [1], and the results of our experiments. We conclude with a summary and prospects for future work.

II. Related Work

Because human-robot collaboration is necessary for advanced automation, planning for a robot while maintaining human safety is an active research topic. Most safety efforts in this area appear to fall into two categories based on whether the robot is assumed to be functioning in an active or passive role when interacting with a human.

In the case where a robot is assumed to be taking an active role, the human is generally considered to take the role of a more passive observer. Planned motions are thus made to be more understandable to the human. For example, [2] aims to generate more human-like motions by first generating a reachability map that is used to choose an ergonomic and understandable goal configuration. Unlike this work, our goal focuses on generating robot trajectories that can avoid human motions in the shared workspace environment. Similarly, [3] takes into account a human's visibility, comfort and reachability in the robot's configuration space. This approach is useful when performing hand-over tasks to a human, however, we focus on applications in which a human and robot perform simultaneous pick-and-place tasks in a shared workspace. Finally, [4] aims to convey manipulation intent by purposefully bending a trajectory to better communicate which goal is being reached for. We focus more on generating robot motions that are consistent and avoid human workspace lanes rather than focusing on conveying human intent through motion generation.

In pick-and-place manufacturing tasks, a human should feel safe enough to work freely in a workspace; giving minimal consideration to its robot counterpart. In this scenario, to maintain safety the robot must take an observational role of the "active" human. As a result, research in this case generally aims to predict a human's future motion. Our previous work [5] uses a library of human motions performed in isolation to create pre-computed Gaussian Mixture Models that are queried on-line to predict a human's future workspace occupancy. [6] uses Inverse Optimal Control to predict a human's motion in human-human collaborations.

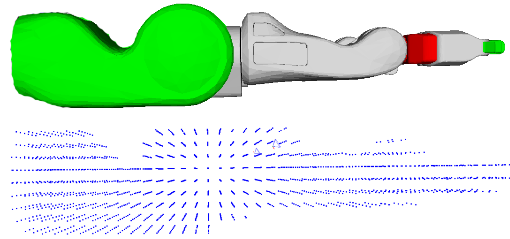

Fig. 2. Example of samples taken on the PR2's manipulator

However, these methods gather human motions either in isolation or in human-human collaboration. In this work the costs functions we create are derived from the human's motion in collaboration with the robot. Koppula et al. [7] used Conditional Random Fields (CRFs) to model affordances of objects and 3D trajectories of the human hand. This work has been recently extended in [8] to predict high-dimensional trajectories. Here we avoid parametric modeling of the human's motion, using the workspace occupancy directly. We also consider the consistency of the robot's motion, which is not addressed in the above methods.

While the principles of human motion have been investigated in [9],[10],[11],[12], these works take a more low-level approach by considering muscle activation or neural activity with respect to motion. However, our approach is more high-level in that we learn regions of the workspace to use or avoid in relation to a human. Our approach thus does not require a complex bio-mechanical model of the human.

Other works such as [13] [14] attempt to account for dynamic obstacles in motion planning. While the human may be considered a dynamic obstacle, we would like to avoid re-planning as much as possible due to its time cost. Our method aims to generate motions that could be used with with a dynamic planner, but we aim to minimize the need for re-planning under the assumption that areas with low human lane penetration cost are likely to be collision-free.

III. Approach

Our approach to generating consistent, human-avoiding reaching motions consists of a voxel based representation of the workspace that records occupancy over time for both a robot and human collaborator. These occupancy grids are used to define two cost functions. The first of these cost functions, the human lane penetration cost, aims to model the avoidance factor by repelling robot configurations from the areas of the workspace that should be reserved for traversal by a human collaborator. The second, the robot self-lane tracking cost, aims to model consistency factor by attracting robot configurations toward previously used areas of the workspace. These cost functions are then used in a trajectory optimizer.

A. *Workspace Modeling*

Our method discretizes the shared workspace into two voxel occupancy grids - $H[i,j,k]$ for the human and $R[i,j,k]$ for the robot, where (i,j,k) is the index of the voxel in the occupancy grids. We define a function $m(\mathbf{p}) = (i,j,k)$ which maps a point $\mathbf{p} = (x,y,z)$ to an index of the voxel in the occupancy grids. Each voxel $H[i, j, k]$ and $R[i, j, k]$ is initialized with an occupancy value of 0.

To update the human and robot occupancy, we first pre-compute a set of samples in the geometry of the each link in the arm of both the human and robot simulation models, as shown in Fig. 2. To model human motions in simulation we use a motion capture system with inverse kinematics to obtain a 23 DoF configuration of the human's head, torso and right arm. Each pre-computed sample, denoted as $\mathbf{p}_i^j$, represents the ith point on the robot/human model link j. At each time step, the transformation matrix T_j^0 between F_j, the frame of link j and F_0, the frame of workspace is computed. We then transform $\mathbf{p}_i^j$ to the workspace frame by $T_j^0\mathbf{p}_i^j$. Thus the human and robot occupancy grids are updated as follows:

$$\begin{cases} H[m(T_j^0\mathbf{p}_i^j)] = H[m(T_j^0\mathbf{p}_i^j)] + 1 & \text{if link } j \in \text{Human} \\ R[m(T_j^0\mathbf{p}_i^j)] = R[m(T_j^0\mathbf{p}_i^j)] + 1 & \text{if link } j \in \text{Robot} \end{cases}$$

This sampling and incrementing of voxels allows areas of the workspace that are used most by their respective grid owners(human/robot) to emerge over time.

B. Human Lane Penetration Cost

In order to generate motions that avoid areas of the workspace used by a human, we define a human lane penetration cost function. The idea comes from the observation and assumption that human motions are always constrained in a subspace of the workspace when the human is working on a set of repetitive tasks in a shared workspace. This constrained subspace is similar to flight lanes used by aircraft. Each aircraft is constrained to a specified lane such that they can avoid each other without considering each other's motion. We likewise model the lanes used by a human through the above occupancy grids. Rather than model human lanes as solid obstacles that the robot needs to avoid completely, we model human lanes as a cost map called lane penetration cost, as the human lanes are not always entirely occupied by the human and the human can also adapt their motions to the robot.

Simply using the raw human occupancy value will assign high cost to configurations that penetrate high use regions of the workspace. However, this approach fails to provide lower cost to configurations far from occupied regions relative to configurations on the boundary of occupied regions. As a result, we employ a combination of the occupancy value, and the Signed Distance Field (SDF) of the human occupancy grid as follows:

$$pen\_cost(H, \mathbf{p}) = occH(H, \mathbf{p})sdfH(H, \mathbf{p}) \tag{1}$$

where $\mathbf{p}$ is any point in the workspace, $occH(H, \mathbf{p})$ produces the normalized occupancy grids value for point $\mathbf{p}$, and $sdfH(H, \mathbf{p})$ is the normalized value of the SDF of the human occupancy grid. The $occH(H, \mathbf{p})$ is defined as:

$$occH(H, \mathbf{p}) \begin{cases} \frac{\log(0.9+1)}{\log(maxH+1)} & \text{if } H[m(\mathbf{p})] = 0 \\ \frac{\log(H[m(\mathbf{p})]+1)}{\log(maxH+1)} & \text{if } H[m(\mathbf{p})] > 0 \end{cases} \tag{2}$$

where $maxH$ is the maximum voxel value across the entire human occupancy grid. We use 0.9 when the voxel value is 0 in order to avoid flat regions of cost for the space outside human lanes, as a flat region has no gradient, which causes problems for the trajectory optimizer. We use the $\log$ function to reduce the influence of the maximum voxel value, as linear normalization of raw voxel values is overly sensitive to the maximum voxel value. Consider an example in which a human is standing at rest for numerous timesteps followed by a quick reaching motion. The voxels which belong to the reaching portion of the trajectory will be normalized to nearly zero cost relative to the maximum cell value recorded for the resting portion of the trajectory. Using a $\log$ here ameliorates this issue. The $sdfH(H, \mathbf{p})$ is defined as:

$$sdfH(H, \mathbf{p}) = \frac{\arctan(maxSH) - \arctan(sdf(H, \mathbf{p}))}{\arctan(maxSH) - \arctan(minSH)} \tag{3}$$

where $sdf(H, \mathbf{p})$ is the function that returns the SDF value for a given occupancy grid and a given query point $\mathbf{p}$. $maxSH$ and $minSH$ are the maximum and minimum SDF value for the human occupancy grids H. $sdf(H, \mathbf{p})$ will return a negative value when $\mathbf{p}$ is inside the occupied volume described in the occupancy grids H, a positive value if $\mathbf{p}$ is outside or 0 if $\mathbf{p}$ is on the boundary. The magnitude is determined by how far $\mathbf{p}$ is from the boundary of the volume, which, in our case, is the outside surface of the lanes. We use the $\arctan$ function to give an upper bound and a lower bound to the SDF value and keep it equal to 0 on the boundry, as we want to reduce the influence of the points far away from the volume. Note that this normalization function results in the most negative value of the SDF (the innermost point in the lane) mapping to 1, and the most positive value of the SDF (the point farthest from the lane) mapping to 0. A two-dimensional slice of the human lane penetration costmap can be seen in Figure 3.

C. Robot Self-Lane Cost

While the lane penetration cost aims to facilitate human workspace avoidance, we also need to consider the consistency of the robot's motion. We define a robot self-lane cost in a similar fashion to the lane penetration cost with the intention of favoring motions which traverse the voxels most used in the robot's occupancy grid. The robot self-lane cost is defined as follows:

$$self\_cost(R, \mathbf{p}) = occR(R, \mathbf{p})sdfR(R, \mathbf{p}) \tag{4}$$

where $occR(R, \mathbf{p})$ and $sdfR(R, \mathbf{p})$ represent the normalized voxel value of robot occupancy grids and normalized SDF value of robot occupancy grids similar to the human lane penetration cost. However, we invert the upper and lower bound of the normalization for each term as the robot self-lane cost is intended to attract the robot while the human penetration cost aims to repel the robot. The $occR(R, \mathbf{p})$ and $sdfR(R, \mathbf{p})$ are defined as follows:

$$occR(R, \mathbf{p}) \begin{cases} 1 - \frac{\log(0.9+1)}{\log(maxR+1)} & \text{if } R[m(\mathbf{p})] = 0 \\ 1 - \frac{\log(R[m(\mathbf{p})]+1)}{\log(maxR+1)} & \text{if } R[m(\mathbf{p})] > 0 \end{cases} \tag{5}$$

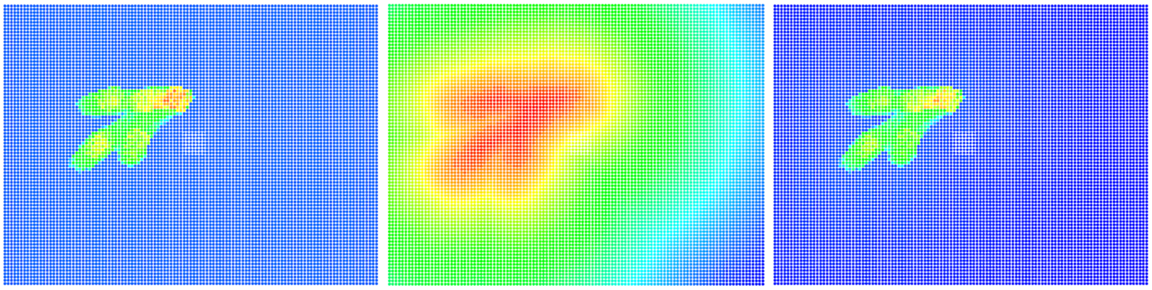

(a) Normalized Occupancy Value (b) Normalized SDF Value (c) Occupancy Value * SDF Value

Fig. 3. A slice of the human lane penetration cost function from simulated data. From left to right, the first figure shows $occH(H, \mathbf{p})$, the second figure shows $sdfH(H, \mathbf{p})$, while the third figure shows the resulting product of both values, $pen\_cost(H, \mathbf{p})$

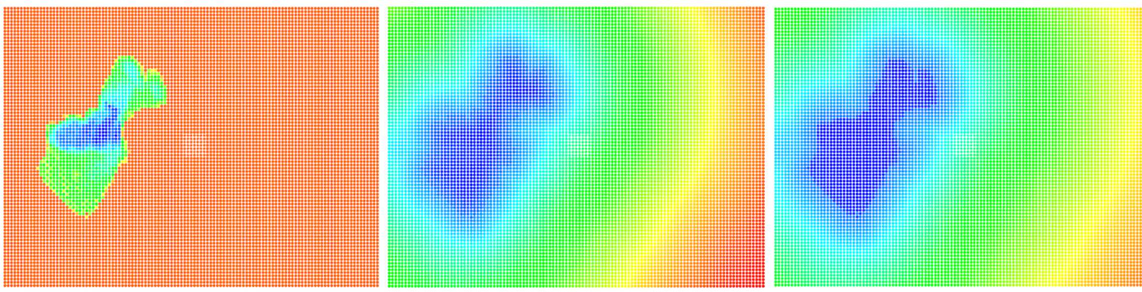

(a) Normalized Occupancy Value (b) Normalized SDF Value (c) Occupancy Value * SDF Value

Fig. 4. A slice of the robot self lane cost function from simulated data. From left to right, the first figure shows $occR(R, \mathbf{p})$, the second figure shows $sdfR(R, \mathbf{p})$, while the third figure shows the resulting product of both values, $self\_cost(R, \mathbf{p})$.

$$sdfR(R, \mathbf{p}) = \frac{\arctan(sdf(R, \mathbf{p})) - \arctan(minSR)}{\arctan(maxSR) - \arctan(minSR)} \quad (6)$$

where $maxR$ is the maximum voxel value of the robot occupancy grid R, and $maxSR$ and $minSR$ are the maximum and minimum SDF value of the robot occupancy grid R. The product of these normalized terms produces 0 cost in voxels most occupied in the center of occupied regions, with a smooth increase in cost of unoccupied regions. A two-dimensional slice of the robot self lane costmap can be seen in Figure 4.

Unlike the human lane penetration cost which accounts for all observed human motion, regardless of the task the human is performing (we do not assume the robot knows which task the human is doing), the robot self-lane cost function aims to model consistency for each task separately. Thus we maintain one robot occupancy grid for each robot task.

D. Robot Trajectory Optimization

We use the TrajOpt [1] sequential convex optimization algorithm to plan with the cost functions described in Sections III-B and III-C. We include collision, final end-effector pose, and maximum end effector displacement constraints as well as a weighted joint velocity cost. After trying a number of different initial trajectories, we found the best initialization was a path consisting of the first $n-1$ configurations as the starting configuration and the lowest-cost inverse kinematics solution for the nth (final) configuration.

The final cost which TrajOpt uses is the weighted sum of all above costs. We manually tuned the weights between different costs using a pre-recorded training dataset. The tuning process aims to find a weighting that is optimal in terms of human lane penetration cost.

IV. Results

In this section we present results illustrating the capability of both of the above cost functions to generate human lane-avoiding and consistent robot reaching motions. We first show our cost functions' ability to generate human lane-avoiding motions in simulation by comparing generated paths to a baseline. Next we test the impact of our cost functions in a human subjects study by comparing robot behavior produced by our cost functions to a baseline in terms of the task completion time and task success rate. We define the baseline for comparison as a straight-line path in the robot's configuration space from the robot's initial configuration to the inverse kinematics solution at the end-effector goal for a given task that is closest to the initial configuration. The baseline thus does not account for any previous observations of the human and would correspond to what the robot would do if it were performing its task without the human. Importantly, these baseline trajectories are optimally-consistent, as they never change for a given task.

A. Recording Method

In order to record human workspace occupancy for simulated and experimental data, we used a Vicon motion capture system. Human subjects wore a suit consisting of four rigid plates and six individual markers which were placed according to biomechanics industry standards [12]. We used as many rigid plates as possible as they provide

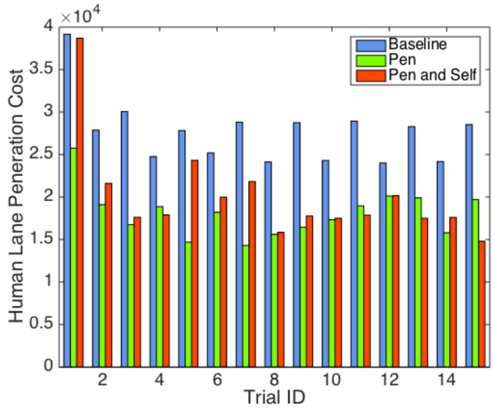

Fig. 5. Comparison of human lane penetration costs for baseline, human lane avoidance (Pen), and human lane avoidance and robot self-lane consistency (Pen and Self) trajectories in simulation

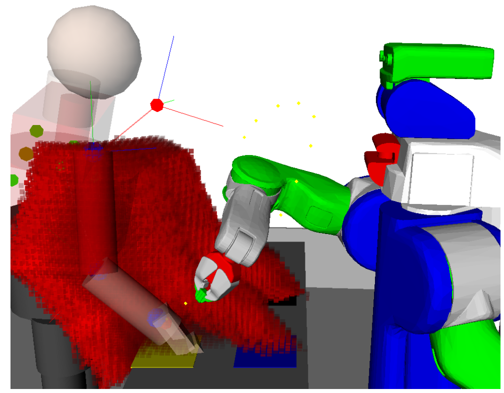

Fig. 6. An example of the human lane penetration cost map. Unoccupied voxels not drawn.

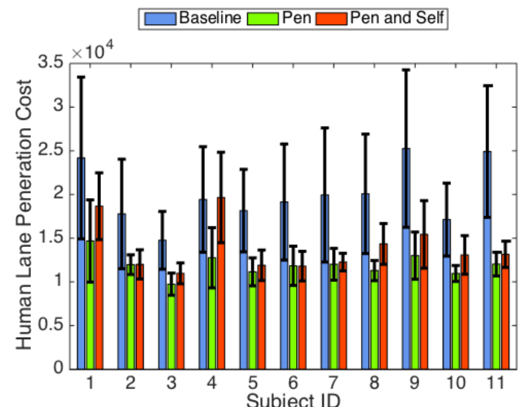

Fig. 7. Comparison of human lane penetration costs for baseline, human lane avoidance (Pen), and human lane avoidance and robot self-lane consistency (Pen and Self) trajectories for each participant in the user study

more robust tracking than their marker counterparts. From our motion capture setup, we extract the center of rotation of the human's right wrist, elbow, shoulder and torso. We obtain a 23 DoF configuration of the human's right arm and torso by performing inverse kinematics with these joint centers.

B. Experiments in Simulation

To evaluate our capacity to optimize trajectories for the presented cost functions, we perform initial comparisons to the baseline method in a simulated environment. Because we are performing this analysis in simulation, we are unable to evaluate the effects of consistent robot motion on a human subject. Instead, in simulation we aim to show that our optimization can produce paths of lower human lane-penetration cost than the baseline method. This analysis is performed in two phases: data collection and planning-in-simulation. (1) In the data collection phase, we record data of a human performing reaching motions to several goals denoted by colored regions on a tabletop. We then manually-segment the recordings into individual reaching motions. (2) In the planning-in-simulation phase, we then place a simulated PR2 robot at the side of the table opposite the simulated human. We then forward-simulate segmented human reaching motions until task completion, recording workspace occupancy of each configuration in the human's motion. We then plan trajectories for the baseline, a trajectory optimized according to Section III-D with the human lane penetration cost (Pen), and a trajectory optimized with both the human lane penetration cost and robot self-lane cost (Pen and Self).

The three methods produce trajectories of varying length. In order to produce a fair comparison between all three types of trajectories, we insert a trajectory resampling step prior to evaluation of a trajectory's penetration cost, so that trajectories are discretized at a fixed step size of $0.05\mathrm{rad}$. The resampling step is necessary because, while the number of waypoints used by TrajOpt is constant, the distance between them is not.

Figure 5 provides a comparison, in terms of human lane penetration cost, of the trajectories produced by the three methods on the example scenario shown in Figure 6. The x axis on the figure shows the sequence of reaching targets for the robot. Note that the voxel grids are updated between the tasks with the human's and robot's previous motion. The results clearly show that optimization with the lane-avoidance cost function produces significant improvements for avoiding lanes over the baseline. Unsurprisingly, if we include the self-lane tracking term in the optimization, the optimizer settles to a solution that trades off self-lane following for avoiding the human's lane, thus we see that the lane-penetration cost of the combined cost function is worse than optimizing for lane-avoidance alone. In most cases, however, the combined cost function still improves over the baseline in terms of avoiding the human's lane.

C. Human-Robot Experiments

While the results performed in simulation demonstrate the capability of both methods to generate trajectories of lower human lane penetration cost than a baseline, it is unclear what effect such robot trajectories will have on a human collaborator. We conducted a human subjects study where a human performed pick-and-place motions while a PR2 performed reaching motions in a shared workspace. We evaluated each method in terms of task completion time and task success rates. These metrics were chosen under the assumption that workspace lane avoiding motions from the robot will make human task execution simpler. To ensure fairness between methods we consider the maximum execution time between subjects and the PR2 as the task completion time.

The experiment was designed so that the robot would need to enter the human's workspace to complete its task and vice versa. The task was for the robot to reach to one of two specified end-effector poses near the human and then return to its initial configuration. Simultaneously, the human was to perform two pick-and-place motions to targets near the robot.

When a human moves at their natural speed, they can perform their task much faster than we can safely execute a robot trajectory, allowing the human to avoid the robot entirely. As a result, we directed participants to place two ping-pong balls balanced on top of 3D printed molds with a slight dimple at two goal positions in sequence without letting the balls roll off the molds. This constrained task required the human to move at a speed comparable to the robot. We define a successful completion of a task as a trial in which both of the molds are placed directly in the predefined goal regions and the ping-pong balls remain balanced on the molds for the duration of execution.

Upon entering the experiment area, subjects were read a script which briefly explained they were to perform a collaborative manipulation task. Next, the task to be performed was verbally explained while being visually demonstrated in unison. Participants were asked to move at a comfortable speed while ensuring balance of the ping pong ball throughout the task. Finally five demo executions were performed to ensure basic task understanding.

After being introduced to the study, one of the three methods was selected at random. The human performed a sequence of twenty executions of the aforementioned task which contained a balanced number of trivial executions in which the PR2 reached to an unrelated area of the workspace as well as conflicting executions in which the PR2 reached to the same area of the workspace as the human (eg. Figure 9). The experimenter initiated the task by telling the human which targets to place the molds on and simultaneously starting the robot's motion for its own target. A run of the experiment was finished when the human and robot both completed their tasks. A new robot trajectory is planned prior to each task execution in the sequence. On average, planning took 4.3ms, 6.82s, 15.39s with a standard deviation of 3.5ms, 2.77s, 5.89s for the Baseline, Pen and Pen+Self methods, respectively. Upon finishing the sequence subjects were asked to play a simple video game for five minutes before continuing to the next randomly selected method. This is designed to encourage subjects to shift their attention away from the robot and thus engage with each method with similar familiarity.

We ran this experiment with 11 subjects, each performing 20 runs of each method generating a total of 660 human reaching trajectories. We had 8 male participants and 3 female participants. The ages of the participants rage from 18 to 25. The median age is 24. Motions generated using TrajOpt were initialized with a trajectory of 12 waypoints as described in Section IV-B. The human lane penetration cost was scaled with $\alpha = 0.7$, the robot self-lane cost with $1-\alpha$, the weighted joint velocity cost was $1000 \times w$ where w is an auto-generated weight vector for the PR2 robot. In addition to this, a maximum displacement of 0.1 meters on end-effector displacement between configurations was used to encourage even spacing of configurations.

Figure 7 shows a comparison of average human lane penetration costs for all three methods for every subject in the experiments. Similar with the simulation results, optimization with the human lane penetration cost alone shows significant improvement in terms of path cost when compared to the baseline. Likewise, except for subject four, motions planned including the robot self-lane cost yield trajectories which outperform the baseline, yet are of slightly higher cost than when optimizing for human lane penetration cost alone.

The benefit of this improvement in lane penetration cost for both of our methods can be seen in Figure 9, in which individual robot configurations are visually compared. In the figure, the robot is executing a task which conflicts with the subject's task. In the case of a trajectory planned with the baseline, the PR2's arm significantly occludes the subject's goal region, necessitating a pause in the subject's motion. Alternatively, trajectories which include the human lane penetration term provide ample room for the subject to execute his or her task fluidly.

Table 8 shows the average task completion time, task success rate and human lane penetration cost for the entire dataset. Both methods slightly outperform the baseline in terms of task completion time. The method which aims to only avoid the human has the lowest execution time while the method with the added robot consistency term has a better task success rate. This is what one would expect as the pure avoidance method would sometimes generate motions that would confuse or alert subjects, causing them to lose balance of the ping-pong ball. Most surprisingly, the optimally consistent baseline method had the lowest success rate of all.

A more detailed break down can be seen in Figure 8 which shows average task completion times and task success rates for each human subject under each method. In every subject excluding subject ten, one of the two methods outperforms the baseline in terms of task completion time, though often by a small margin. Additionally, the Pen+Self method consistently outperforms the baseline and Pen method in terms of task success rates. While the improvements of our methods over the baseline may seem modest, it is important to note

Method	Task completion Time	Task Success Rate	Cost
Baseline	6.94 ± 1.21 s	0.8591 ± 0.1443	$2.00e4 \pm 7.33e3$
Pen	6.62 ± 1.23 s	0.9318 ± 0.0777	$1.19e4 \pm 2.57e3$
Pen+Self	6.71 ± 1.17 s	0.9591 ± 0.0668	$1.39e4 \pm 3.81e3$

TABLE I

COMPARISON OF AVERAGE TASK SUCCESS RATE, PATH COST, AND TASK COMPLETION TIME FOR EACH METHOD OVER 11 SUBJECTS EACH PERFORMING 20 TASK EXECUTIONS

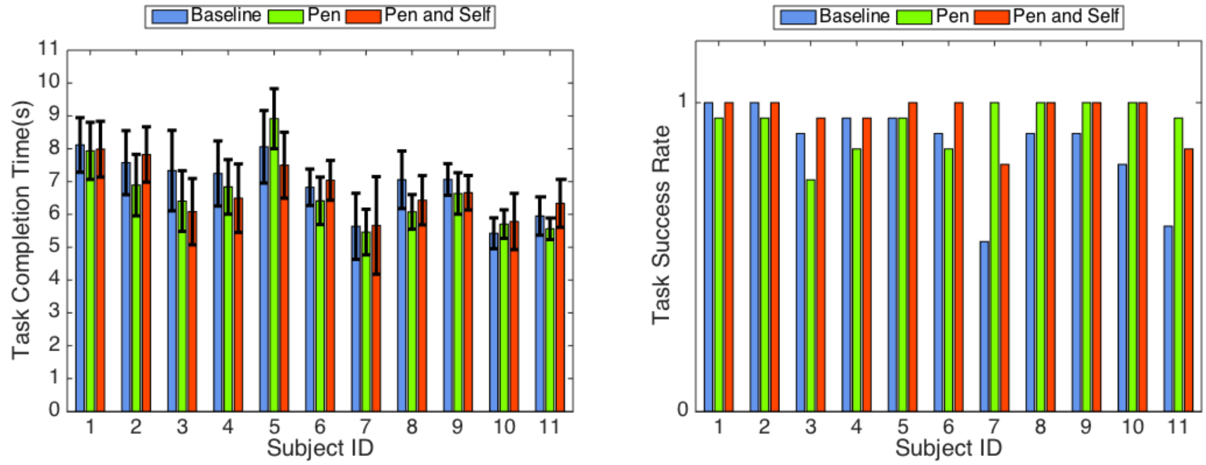

Fig. 8. Comparison of task completion times (left) and task success rates (right) for baseline, human lane avoidance(Pen), and human lane avoidance and robot self-lane consistency(Pen and Self) trajectories for each participant in the user study

Fig. 9. A comparison of robot configurations generated by the baseline method (left) and the avoidance-only method (right). The baseline method is occluding the human's goal region while the avoidance-only method leaves the goal region open.

that these are elementary reaching tasks and that many such motions need to be performed in the course of a practical manufacturing task (e.g. assembly), so the time savings can add up to substantial amounts. Task errors, such as dropping the ball, are especially important to avoid as they would require the human to recover from the error and repeat the task, thus requiring more time.

V. Conclusion

In this work we have presented two cost functions for generating safer motions within proximity to a human in a shared workspace. These costs aim to model avoidance of regions of the workspace that are of importance to human task manipulation, as well consistency in robot motion; factors which were identified as important to human manipulation through observation of human collaboration. To demonstrate the efficacy of the proposed cost functions we provide both simulated results as well as results from a human subjects study. We found that using either cost function we outperform the baseline method in terms of task success rate without degrading the task completion time and the cost function that aims to produce consistent robot motion while avoiding the human produces the highest success rate. These results suggest that the proposed cost functions do indeed improve the efficiency of human robot collaboration in shared workspaces. In future work we aim to study the effects of collaboration strategies on users with different collaboration preferences (e.g. leading vs. following).

VI. Acknowledgements

This work was supported in part by NSF grant IIS-1317462.

References

[1] J. Schulman, Y. Duan, J. Ho, A. Lee, I. Awwal, H. Bradlow, J. Pan, S. Patil, K. Goldberg, and P. Abbeel, "Motion planning with sequential convex optimization and convex collision checking," *IJRR*, vol. 33, no. 9, pp. 1251–1270, Aug. 2014.

[2] F. Zacharias, C. Schlette, F. Schmidt, C. Borst, J. Rossmann, and G. Hirzinger, "Making planned paths look more human-like in humanoid robot manipulation planning," in *ICRA*, May 2011.

[3] J. Mainprice, E. Sisbot, L. Jaillet, J. Cortes, R. Alami, and T. Simeon, "Planning human-aware motions using a sampling-based costmap planner," in *ICRA*, May 2011.

[4] A. Dragan and S. Srinivasa, "Generating legible motion," in *Robotics: Science and Systems*, June 2013.

[5] J. Mainprice and D. Berenson, "Human-robot collaborative manipulation planning using early prediction of human motion." in *IROS*, Nov 2013.

[6] J. Mainprice, R. Hayne, and D. Berenson, "Predicting human reaching motion in collaborative tasks using inverse optimal control and iterative re-planning," in *ICRA*, May 2015.

[7] H. S. Koppula and A. Saxena, "Anticipating human activities using object affordances for reactive robotic response." RSS, 2013.

[8] Y. Jiang and A. Saxena, "Modeling high-dimensional humans for activity anticipation using gaussian process latent crfs," in *Robotics: Science and Systems, RSS*, 2014.

[9] T. Flash and N. Hogan, "The coordination of arm movements: an experimentally confirmed mathematical model," *The journal of Neuroscience*, vol. 5, no. 7, pp. 1688–1703, 1985.

[10] E. Burdet and T. E. Milner, "Quantization of human motions and learning of accurate movements," *Biological cybernetics*, vol. 78, no. 4, pp. 307–318, 1998.

[11] E. Demircan, T. Besier, S. Menon, and O. Khatib, "Human motion reconstruction and synthesis of human skills," in *Advances in Robot Kinematics: Motion in Man and Machine*. Springer, 2010, pp. 283–292.

[12] Wu and et al, "Isb recommendation on definitions of joint coordinate systems of various joints for the reporting of human joint motion – part ii: shoulder, elbow, wrist and hand," *Journal of biomechanics*, vol. 38, no. 5, pp. 981–992, 2005.

[13] C. Park, J. Pan, and D. Manocha, "Real-time optimization-based planning in dynamic environments using gpus," in *ICRA*, 2013.

[14] O. Brock and O. Khatib, "Elastic strips: A framework for motion generation in human environments," *The International Journal of Robotics Research*, vol. 21, no. 12, pp. 1031–1052, 2002.